RESEARCH ARTICLE-CIVIL ENGINEERING

Numerical Simulation of Ventilation Performance for Large-scale Underground Cavern Group Considering Effect of Ventilation Shaft Structure

Yimin Xia[1,2] · Xuemeng Xiao[1,2] · Yazhou Zhang[3] · Shuying Wang[4] · Laikuang Lin[1,2]

Abstract

Construction ventilation runs through the entire construction process of large underground caverns and is the key to ensuring construction progress and project safety. For the specific underground cavern group of pumped-storage power plants, a three-dimensional model is constructed, and the *CFD* method based on fluid mechanics theory is used to simulate the ventilation flow field of the underground cavern group. Through the comparison of the airflow in the main caverns and the air velocity distribution law, Quantitative analysis of the influence of the diameter of the ventilation shaft and the inclination of the shaft on the ventilation flow field shows that when the diameter of the ventilation shaft is 8 m and the inclination of the shaft is 80°, the ventilation effect in the underground cavern group is the best. Applying this scheme to engineering practice and conducting on-site tests, the average relative error of the measuring points is 11.32% by comparing the measured data and the simulation results, which verifies the correctness of the *CFD* method used. It provides reference value for studying the construction ventilation of underground caverns.

Keywords Underground cavern group · Construction ventilation · Numerical simulation · Air velocity distribution · Ventilation shaft

1 Introduction

Large-scale underground caverns have many construction tunnels, with complex and diverse structures. The tunnels are connected to each other, and the main caverns have long ground passages and tortuous lines which makes it very difficult to ventilate and disperse smoke during the construction period. Good construction ventilation is directly related to the construction efficiency, construction progress and safety of the cavern group, as well as the health of the operators. Therefore, the construction ventilation of the cavern group plays an important role in the construction plan and construction schedule of the whole project [1].

At present, the ventilation performance of underground space is mainly studied by the following three methods: full-scale experiment investigation, reduced-scale test and numerical simulation [2]. Among them, the full-scale investigation can obtain more ideal data since it is close to practice most and can reproduce the actual operating conditions of ventilation process in the underground space. Tong et al. [3], Zhong et al. [4, 5], Sun et al. [6] conducted a full-scale fire field test to reveal the flow of smoke in the tunnel under actual fire conditions. Pflitsch et al. [7] found the law of airflow in the tunnel through actual measurement of the air velocity, temperature and thermal image in the subway tunnel. Due to the large scale of underground space, full-scale experimental research is expensive and time-consuming. In contrast, numerical simulation methods have been adopted by many scholars for their reliability, rationality and convenience. Musto et al. [8], Nan et al. [9], Lee et al. [10] used numerical simulation to study the influence of jet fan

✉ Xuemeng Xiao
604842099@qq.com

1   College of Mechanical and Electrical Engineering, Central South University, Changsha 410083, China

2   State Key Laboratory of High Performance Complex Manufacturing, College of Mechanical and Electrical Engineering, Central South University, Changsha 410083, China

3   China Railway 14Th Bureau Group, Shield Engineering Co., LTD, Nanjing 211899, China

4   School of Civil Engineering, Central South University, Changsha 410083, China

parameters on the tunnel ventilation system. Diego et al. [11] proposed a method to calculate the air loss in tunnels of arbitrary geometry. Wang et al. [12] studied the flow field distribution and pressure distribution in the diversion tunnel. The simulation results show that the airflow rate, flow rate and air leakage rate gradually decrease along the tunnel, and there is a low pressure area near the air leakage area. Sa et al. [13] established the dust migration model in the cavern's stope according to the gas–solid two-phase flow theory and the characteristics of the cavern group and used Fluent software to simulate the distribution of dust concentration after blasting and the dust trajectory at different wind velocity. Zhang [14], Lin [15], and Hua [16] used numerical simulation method to study the ventilation flow field in the underground cavern and proposed reasonable optimization schemes.

The above research has mainly focused on the ventilation performance during the excavation of a single tunnel, but there are very few research on the composite ventilation between multiple tunnels after the excavation of the cavern group being finished. In fact, due to the crisscross and complex structure of the underground caverns, the airflow between the caverns affects each other, so the rationality of the ventilation design needs to be considered as a whole [17].

Based on computational fluid dynamics and modern testing technology, the paper establishes a simulation model of the overall ventilation flow field of the underground cavern group and uses the CFD method to analyze the wind field distribution in the cavern group under different ventilation

shaft parameters. Finally, the effectiveness of the simulation model is verified by the results of speed testing. This research is helpful to grasp the actual ventilation effect of the cavern group, realizes the optimal configuration of ventilation resources and provides a basis and reference for the ventilation design of similar projects.

2 Background

2.1 Project overview

The underground cavern group of the Jixi pumped storage power station is mainly composed of diversion tunnels, diversion surge chamber, penstock, diversion bifurcation, main powerhouse, main transformer room, busbar chamber, drainage gallery, draft tube gate chamber, tailrace tunnel, traffic tunnel, ventilation and safety tunnel. The structure of the underground cavern group is shown in Fig. 1. The cross-sectional shape and dimensions of the main caverns are shown in Fig. 2.

2.2 Ventilation scheme

In the third ventilation phase of the Jixi pumped storage power station, the excavation of underground cavern group has been basically completed, and the water diversion system, the three large caverns (the main powerhouse, the main transformer room and the draft tube gate chamber) and tailrace system have been connected together, entering
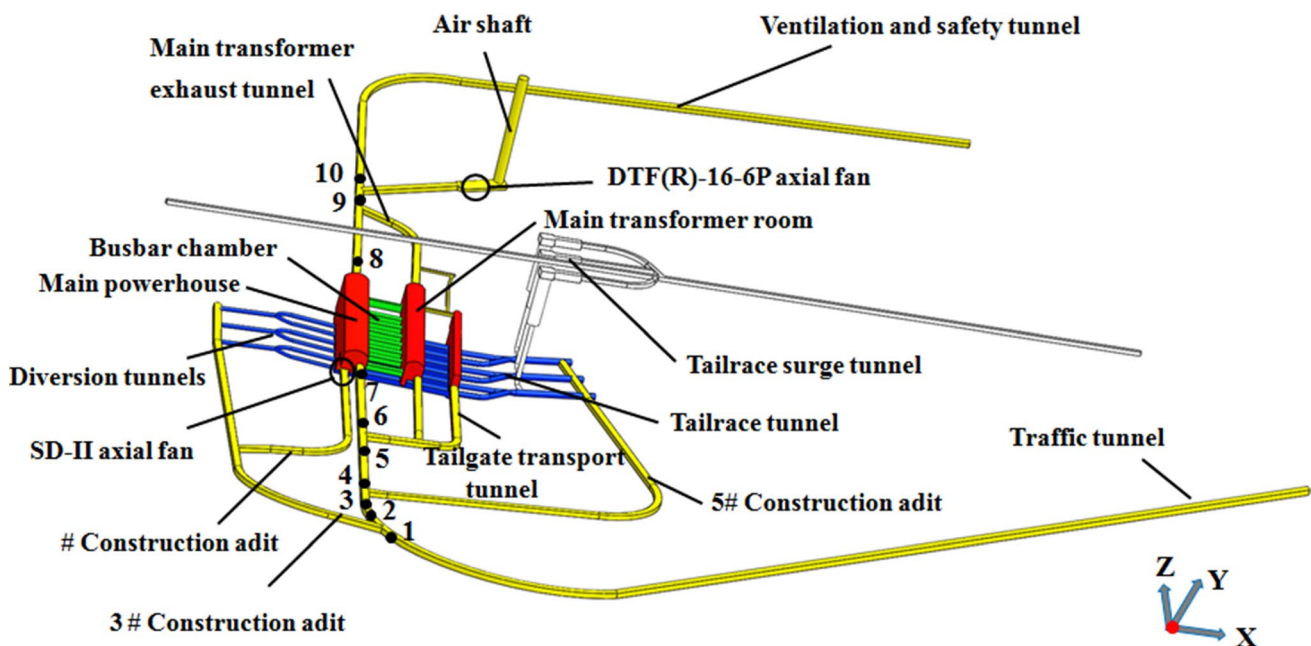

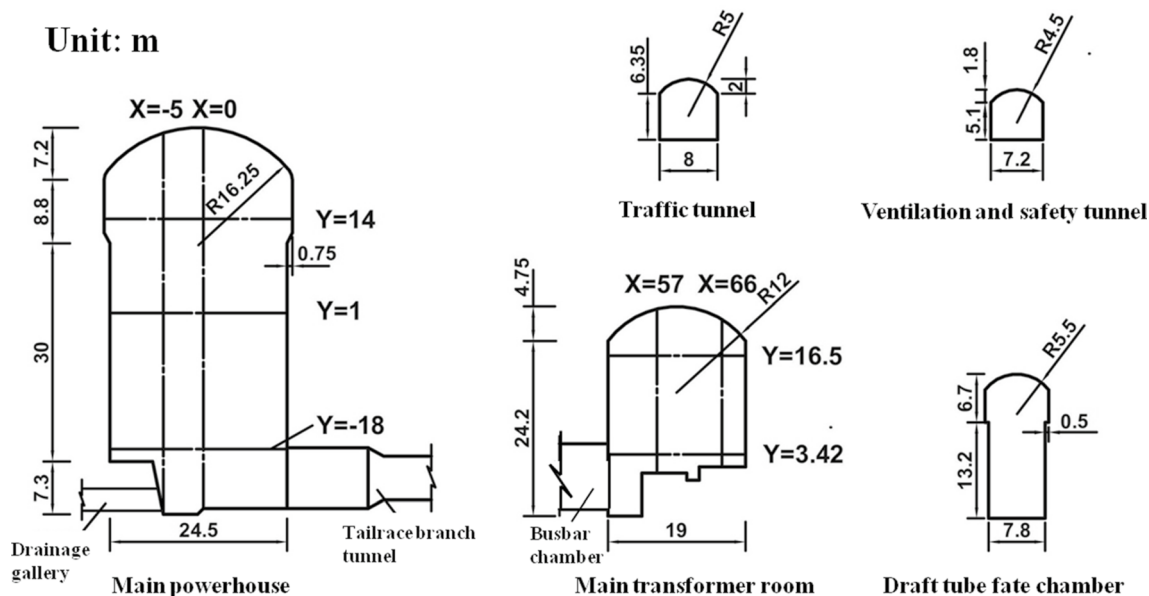**Fig. 1** Structure of underground cavern group

Fig. 2 Section shape and size of main caverns

the stage of concrete lining, grouting and mechanical and electrical equipment installation. The airflow between different caverns interferes with each other, and the distribution of air velocity field is complicated, which brings many difficulties to the discharge of polluted air. It is necessary to design the ventilation scheme reasonably. Therefore, in order to improve the construction ventilation environment, the ventilation shaft is constructed as the exhaust passage of the polluted air. Based on the principle of gallery ventilation, the ventilation scheme is designed as follows:

The ventilation scheme is based on natural ventilation, supplemented by the mechanical ventilation. The traffic tunnel is used as fresh air inlet, and the ventilation shaft serves as outlet of the polluted air. The airflow between different caverns interferes with each other since the tunnels are intersecting. The distance between the entrance of the traffic tunnel and the main powerhouse is close to 1.7 km, thus it is difficult to meet the ventilation requirements only by natural ventilation, so the mechanical ventilation is needed to strength the ventilation effect. A *SD-II* axial fan is arranged to supply air at the intersection of the main powerhouse and the 4# construction branch tunnel, and a *DTF(R)-16-6P* axial fan is arranged at the bottom of the ventilation shaft to discharge the polluted air.

2.3 Research approach

In this paper, based on the underground cavern group of a pumped storage power station, the parameters of the ventilation shaft built in it are studied in depth. Firstly, a 1:1 three-dimensional model of the cavern group was established, and

the mesh was divided. Then, a basic numerical model was established based on the basic assumptions of the cavern group and the mathematical model to be followed. Secondly, according to the specific working conditions and actual test data, the boundary conditions are set to study the influence of the diameter of the ventilation shaft and the inclination of the ventilation shaft on the ventilation effect, so as to determine the better ventilation effect scheme, and the ventilation performance evaluation is carried out. Finally, this scheme is applied to the actual project, and the field wind speed test is performed on the actual underground caves, and the test results are verified with the simulation results to verify the correctness of the numerical model. The technical roadmap is shown in Fig. 3.

3 Basic simulation

3.1 Basic assumptions

(1) The airflow in the underground cavern group is viscous, incompressible and turbulent fluid.
(2) The airflow is evenly distributed at the entrance of the tunnels and the outlet of the fan, and the ventilation system runs stably.
(3) The tunnel wall is Adiabatic, and there is no heat source in the computational domain and the temperature change of the airflow in the process of ventilation is no considered.
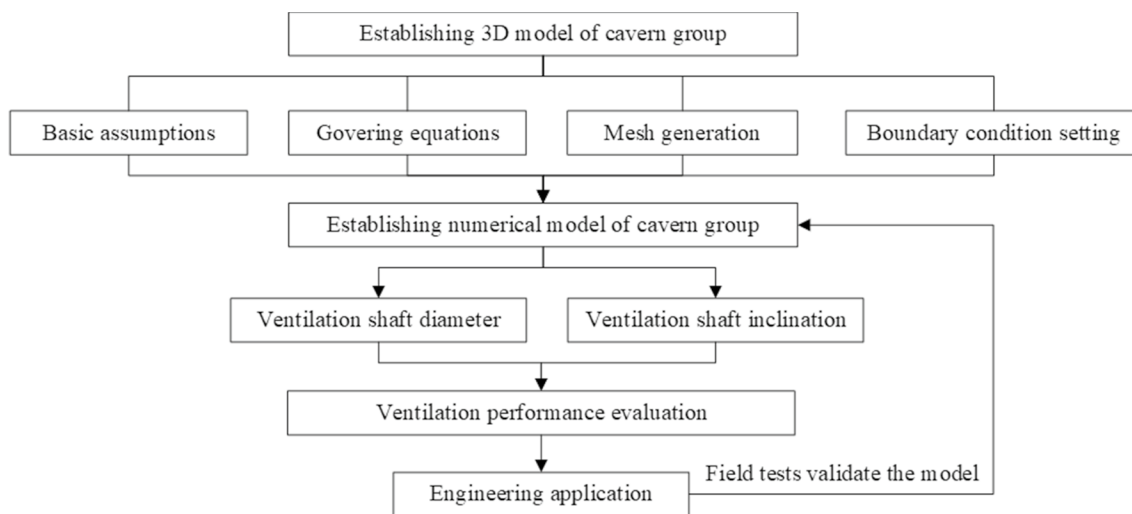
Fig. 3 The technical roadmap

3.2 Governing equations

The airflow in the large underground cavern group mainly follows the law of mass conservation, momentum theorem, the law of conservation and transformation of energy, etc. The governing equation is shown as follows:

Continuity equation:

$$\frac{\partial \rho}{\partial t} + \nabla \cdot \rho U = 0 \tag{1}$$

Navier–Stokes equations:

$$\rho \left[\frac{\partial u}{\partial t} + U \cdot (\nabla U) \right] + \nabla p = \nabla \cdot \tau + S_M \tag{2}$$

Energy conservation equation:

$$\frac{\partial}{\partial t}(\rho T) + \nabla \cdot (\rho U T) = \nabla \cdot (k \nabla T) + S_E \tag{3}$$

where ρ is the air density, $U = (u, v, w)$ is the airflow velocity, p is the airflow pressure, τ is the viscous stress, S_M is the generalized source term of the momentum equation, T is the temperature, k is the air heat conductivity, S_E is the source term of the energy equation.

The airflow in the underground cavern group is typical turbulent flow. At present, the most popular turbulence model is the two-equation model, among which the standard k-ε model is widely used for its robustness, economy and high accuracy to various turbulence. However, the standard k-ε model is only effective for complete turbulence. In contrast, the *RNG* k-ε model takes turbulent vortices into account and has great advantages in predicting near-wall flow and low Reynolds number flow, performing well in terms of accuracy and efficiency [18]. Therefore, the *RNG*

k-ε model is used to simulate ventilation in underground cavern group. The turbulence energy k and turbulence energy dissipation rate ε are obtained from the following transport equation [19, 20].

$$\frac{\partial}{\partial t}(\rho k) + \frac{\partial}{\partial x_j}\left(\rho u_j k\right) = \frac{\partial}{\partial x_j}\left(\alpha_k \mu_e \frac{\partial k}{\partial x_j}\right) + G_k + G_b - \rho\varepsilon + S_k \tag{4}$$

$$\frac{\partial}{\partial t}(\rho\varepsilon) + \frac{\partial}{\partial x_j}\left(\rho u_j \varepsilon\right) = \frac{\partial}{\partial x_j}\left(\alpha_\varepsilon \mu_e \frac{\partial \varepsilon}{\partial x_j}\right) + C_{\varepsilon 1} C_k \frac{\varepsilon}{k} - C_{s2}\rho\frac{\varepsilon^2}{k} + R \tag{5}$$

where $\mu = \mu_l + \mu_t$ is the effective turbulent viscosity, μ_l is the kinetic viscosity coefficient, μ_t is the turbulent viscosity coefficient; G_k is the turbulent kinetic energy generated by the average velocity gradient; G_b is the turbulent kinetic energy generated by buoyancy; α_k and α_ε are the anti-effective Prandtl numbers of k and ε, respectively; $C_{\varepsilon 1}$ and $C_{\varepsilon 2}$ are the constants with the values of 1.42 and 1.68, respectively.

3.3 Physical model

The 3D model of underground cavern group was established according to 1:1, and the coordinate origin was located at the center of the left wall in the main powerhouse, which is shown in Fig. 1. The following simplifications are adopted for the convenient of solid modelling and mesh generation: the jet fans are simplified to a standard cylinder. The transportation vehicles and construction equipment are ignored considering that their shape is relatively small compared to the underground cavern group.

The unstructured grid is adopted in the computational domain for the complicated and irregular shape of the underground cavern group. The computational domain is

divided into several subregions according to different size of caverns, in which different meshing parameters are set. The local mesh refinement is conducted due to the complex flow field near the intersection of different caverns. On the premise of not affecting the calculation results, the meshing was performed after considering the calculation accuracy and calculation time. The total number of elements of the model is 4438782, and the numerical mesh of the part of the underground cavern group is as shown in Fig. 4.

There are many ventilation inlet and outlet in the underground cavern group, and the airflow characteristics near each inlet and outlet are different, so it is necessary to reasonably set the boundary conditions according to the actual situation [21]. The specific setting of boundary conditions in the numerical simulation model is as follows:

No-slip boundary condition is applied to the tunnel wall and fan surface in which different roughness heights are set, respectively: The surface of the fan is regarded as the metal pipe-wall with the roughness absolute height of 0.0001 m and the roughness constant of 0.5. The absolute height of roughness and the roughness constant of the tunnel wall is set to 0.01 m and 0.5, respectively[22, 23]. Velocity entrance boundary conditions are adopted at the entrance of traffic tunnel, the ventilation and safety tunnel and the downstream of tailrace surge chamber. The entrance velocity is set to 1.18 m/s, 1.36 m/s and 1.75 m/s, respectively, according to the monitoring results of construction site. The pressure outlet boundary condition is adopted at the top of the ventilation shaft.

4 Result and Discussions

Under the current ventilation scheme, the ventilation shaft serves as the main passage to discharge the polluted air, which has an important influence on the overall ventilation performance in the underground cavern group. Therefore, the above model is used to simulate the airflow characteristics of the underground cavern group, and the optimal arrangement parameters of the ventilation shaft are explored.

4.1 Effects of Ventilation Shaft Diameter

The diameter of the ventilation shaft is taken as 6 m, 7 m, 8 m and 9 m, respectively, considering the actual construction requirements, transportation equipment and safety space. At present, the construction is mainly concentrating in the main powerhouse and the main transformer room, based on concrete lining, grouting and electromechanical equipment installation. Therefore, the subsequent analysis mainly focuses on the airflow in the two caverns.

The airflow in the bottom area of the cavern has a great impact on the health and safety of the ground workers. Therefore, the study was conducted by establishing planes at the respiratory zone height (1.4 ~ 1.7 m, 1.5 m here) [24, 25] of the main powerhouse and the main transformer room, respectively. The location of the cross sections in this part and in the following research are shown in Fig. 2. The distribution characteristics of airflow velocity are shown in Fig. 5, where d represents shaft diameter.

As shown in Fig. 5(a), the peak velocity under the four diameters appears in the middle of the plane. When the shaft diameter is 6 m, the inlet fan jet has a smaller influence on
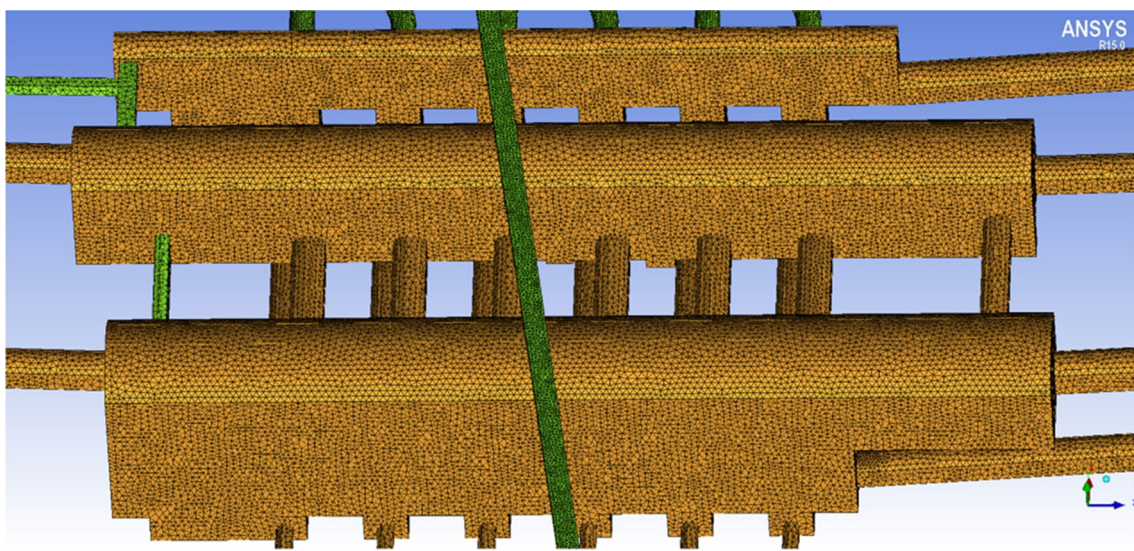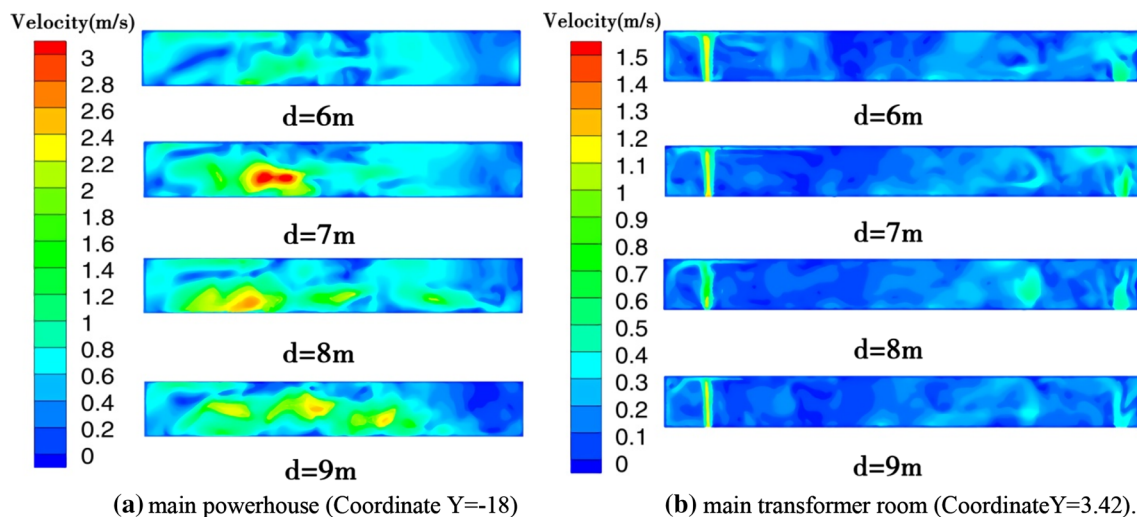

Fig. 4 Numerical mesh of the underground cavern group

Fig. 5 Flow velocity distribution at an elevation of 1.5 m from the ground (d stands for shaft diameter) **a** main powerhouse (Coordinate Y = − 18) **b** main transformer room (Coordinate Y = 3.42)

the original flow field in the main powerhouse. There is a large range of low velocity zone, and the average flow speed is 0.67 m/s. When the diameter of the shaft is greater than 6 m, the influence scope of the jet flow is increased, and the area of the low velocity is obviously decreased, in which case the average flow velocity of the plane is increased to 0.89 m/s, 0.94 m/s and 0.88 m/s, respectively. As shown in Fig. 5(b), for the main transformer room, the airflow velocity in most areas under different diameters is higher than the minimum of 0.15 m/s specified in the "Code for Construction of Underground Excavation of Hydraulic Structures." There is no significant difference in flow velocity distribution under different diameters, indicating that the change in shaft diameter has a limited effect on ventilation in the main transformer room. The airflow velocity in the main transformer room is much lower than the airflow velocity in the main powerhouse. The main reason is that the inlet fan is arranged at the bottom of the main powerhouse, which can effectively increase the airflow velocity in the tunnel. The ventilation in the main transformer cavern is mainly based on natural ventilation, which is less affected by the fan jet flow, thus the airflow velocity is lower.

In order to quantitatively compare the ventilation performance under different shaft diameters, the velocity non-uniform coefficient is introduced to evaluate the uniformity of the velocity distribution in the working area of the cavern. The velocity non-uniform coefficient Kv is defined by Eq. (6) [26, 27]:

$$K_v = \frac{K_v}{\bar{v}} \tag{6}$$

$$\sigma_v = \sqrt{\frac{\sum_{i=1}^{n} (v_i - \bar{v})^2}{n}} \tag{7}$$

where σ_v is the root-mean-square deviation of velocity and $\bar{v}$ is the average flow velocity.

Obviously, the smaller the value of the velocity non-uniform coefficient Kv is, the more uniform the air distribution is. The calculation results of Kv in the two caverns are shown in Table 1. When the airflow in the cavern reaches steady state, the average velocity on the 1.5 m elevation plane in the main powerhouse is the largest when the shaft diameter is 8 m, which are 0.94 m/s. From the perspective of uniformity of flow velocity distribution, the velocity non-uniform coefficient in the main powerhouse decreases with the increase of shaft diameter, and when the shaft diameter is 8 m and 9 m, the uniformity of air distribution in the main

Table 1 The velocity non-uniform coefficient in the main powerhouse and the main transformer room

Tunnel	Diameter(m)	Average velocity (v/m·s⁻¹)	Velocity non-uniform coefficient
Main powerhouse	6	0.67	0.82
	7	0.89	0.78
	8	0.94	0.76
	9	0.88	0.73
Main transformer room	6	0.20	0.76
	7	0.19	0.75
	8	0.20	0.76
	9	0.17	0.77

powerhouse is good. The ventilation in the main transformer room is similar under different cases.

Conclusively, the increase of the ventilation shaft diameter with a certain range is beneficial to the ventilation of the main powerhouse considering that the ventilation shaft is the only outlet of the underground cavern group. And the change of ventilation shaft diameter has little influence on the ventilation performance in the main transformer room. However, due to the complexity of the airflow path in the underground cavern group, the ventilation effect does not always improve with the increase of the diameter of the shaft. According to the simulation results, when the shaft diameter is 8 m, the high airflow velocity as well as uniform velocity distribution can be achieved.

4.2 Effects of ventilation shaft inclination

In underground engineering, the inclination angle of the ventilation shaft is generally 45–90°. The inclination angles of ventilation shaft α are set as 50°, 60°, 70°, 80° and 90°, respectively, which the shaft is the same length. Then, the effect of different shaft inclination angle on the ventilation performance of underground cavern group is analyzed. In order to visually reflect the change of jet flow under different shaft inclination angles, take a point every 10 m along the centerline of the fan and calculate the velocity. The velocity change curve of the jet flow center is plotted in Fig. 6.

As shown in Fig. 6, the velocity of the jet flow drops rapidly after being emitted from the fan. Then, the velocity rises slightly after the flow of 120 m, which is caused by the backflow when the jet flow moves to the wall of the main powerhouse. When the inclination angle of the shaft α is 50° and 90°, the air velocity at the center of the fan jet flow is
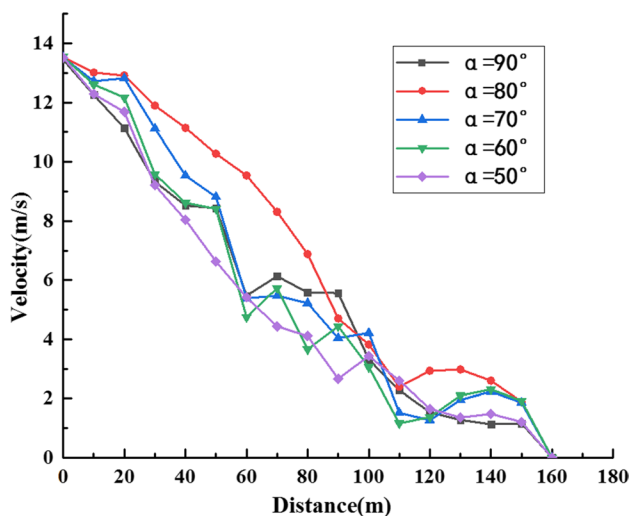
at a lower speed and attenuates faster. And the entrainment effect of the jet flow at a lower velocity on the surrounding air is weaker, which is not conducive to the improvement of the ventilation performance in the underground cavern. Taking a cross section at the center of the fan in the main powerhouse, the velocity distribution is shown in Fig. 7 when the inclination angles of the shaft α are 60°, 70° and 80°. It can be seen from the figure that the form of the fan jet flow is different under different inclination angles. When the inclination angle of the shaft is 80°, the airflow from the fan can form a stable jet flow to move forward, and the jet flow boundary continuously increases and extends until to the end of the main powerhouse. The high speed range of the jet flow (velocity ≥ 10 m/s) is more than 60 m.

The velocity non-uniform coefficients of the two caverns are shown in Table 2. For the main powerhouse, the inclination angle of the shaft has a great influence on the uniformity of velocity distribution. When the inclination angle of the shaft is 60 and 80°, the velocity non-uniform coefficient is small. And for the main transformer room, there is little difference in the velocity non-uniform coefficient of velocity in the five cases. When the inclination angle of the shaft is 70 and 80°, the velocity non-uniform coefficient is small.

Due to in the five cases the ventilation shaft length is the same while the vertical height of the shaft is different,
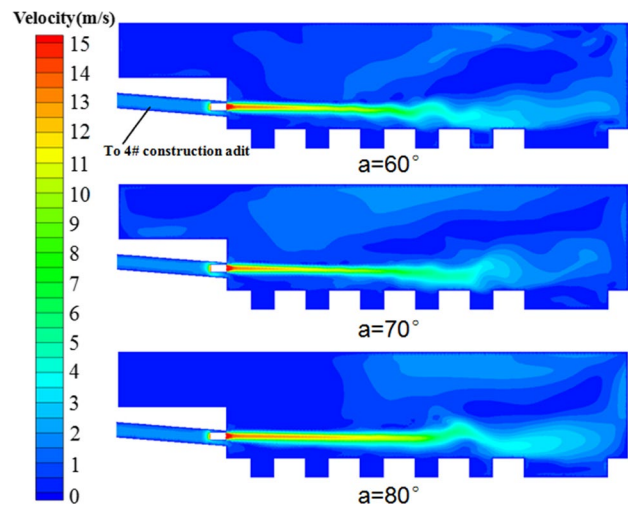

Fig. 7 Velocity distribution on the cross section in the main powerhouse (the section $X = -5$ m)

Fig. 6 Flow velocity on the fan centerline along the tunnel (α stands for inclination angles of ventilation shaft)

Table 2 The velocity non-uniform coefficient in the main powerhouse and the main transformer room

Inclination angle	50°	60°	70°	80°	90°
Main powerhouse	0.70	0.63	0.75	0.65	0.81
Main transformer room	0.74	0.76	0.70	0.72	0.78

so that the pressure difference between the top and the bottom of the shaft is different. At the same time, different ventilation shaft angles directly affect the local resistance coefficient at the corner from the horizontal tunnel to the ventilation shaft, resulting in different local resistance of airflow through the corner. Therefore, the ventilation perform in the five cases are different under the combined action of the above two factors. According to the simulation results, when the inclination angle of the ventilation shaft is 80°, the fan jet flow has a higher velocity and the farthest diffusion distance, which can effectively increase the airflow speed, promote the discharge of the polluted air and improve the air quality of the respiratory zone. Meanwhile, the velocity non-uniform coefficients in the main powerhouse and the main transformer room can also reach the lower levels of 0.65 and 0.72, respectively.

4.3 Ventilation Performance Evaluation

Based on the above analysis, when the diameter of the ventilation shaft is 8 m and the inclination angle is 80°, the ventilation system can reach optimal performance. However, the design of the ventilation shaft should not only consider the ventilation effect, but also consider the geological conditions, civil construction costs, construction conditions and other factors. Therefore, in practical applications, the diameter of the ventilation shaft is finally determined to be 7.7 m. Then, the ventilation performance of the actual working conditions was evaluated by the numerical simulation.

Velocity field distribution is one of the key characteristic of the fluid dynamics analysis [28]. Cross sections are set up at different position to obtain airflow velocity distribution in the main powerhouse and the main transformer cavern, as shown in Fig. 8. The flow field in the main powerhouse is characterized by high flow velocity at the bottom and low flow velocity at the middle and upper part. The average airflow velocity from the top to the bottom is 0.67 m/s, 0.52 m/s and 0.78 m/s, respectively, meeting the requirements of ventilation specifications. The main reason for the higher velocity in the bottom plane is that the plane is closer to the fan jet flow. As the jet flow flows forward, the influence region of the jet flow increases, thus the high velocity area expands continuously. The main transformer room is less affected by the inlet fan jet flow, and its airflow velocity is significantly lower than that in the main powerhouse. The average flow velocity in the two planes is 0.19 m/s and 0.11 m/s, respectively. It can be obtained from the previous analysis that the existence of airflow velocity difference between the two caverns leads to the transverse flow through the busbar chamber, which makes the flow field distribution in the main transformer room slightly disordered.

To further study the effect of fan jet flow on the distribution of flow field, the velocity vector in the cross section in main powerhouse and main transformer room is presented in Fig. 9. As the upper and lower airflows have opposite directions and different speeds, vortices is formed in the middle of the main powerhouse, and the position of the vortex area changes with respect to different sections. According to Zhang Heng [14]、Wang Min. [29], some pollutants will circulate in the vortex area, and take a long time to dilute and discharge, which has adverse effects on the discharge of polluted air. It can be seen from Fig. 9 (b) that the fresh air from the traffic tunnel flows longitudinally, reaching the end of the main transformer room and then flowing out through the ventilation and safety tunnel.

According to the analysis above, the reasonable ventilation path that fresh air is supplied through the bottom branch tunnel and polluted air is discharged through the upper branch tunnel can be formed under the current ventilation scheme, which is conductive to the discharge of pollutants and the replacement of air. And the airflow velocity generally meets the ventilation requirements. Since the airflow distribution in the main transformer room is slightly disordered, it is suggested that the busbar chamber can be closed in the follow-up construction to avoid the transverse airflow in the two caverns.

5 Field Test

In order to truly evaluate the ventilation effect in the underground caverns, measuring points are located near the intersection of caverns at 1.5 m from the ground in the middle of the caverns, as shown in Fig. 1. The airflow velocity in measuring points is measured for 30 s at the construction site and averaged. The measuring instrument is AR866 hot-wire anemometer, with a measuring range of 0–30 m/s and an accuracy of ± 5% + 1dgt. Figure 10 shows the field photograph of the application effect of the actual ventilation scheme. As shown in the figure, the air quality in the main powerhouse and the main transformer room is good.

The airflow velocity at each measuring point is calculated by the established simulation model and compared with the measured data to verify the feasibility and accuracy of the simulation model in this paper. The comparison between the numerical simulation results and the field data of airflow velocity at measuring points is shown in Fig. 11. As can be seen from the figure, along the direction of the traffic tunnel—main powerhouse—ventilation and safety tunnel, the numerical simulation results of airflow velocity is roughly the same as the field data, with an average relative error of 11.32%. The simulation value basically coincides with the measured value, which proves the accuracy of the numerical

Fig. 8 Velocity distribution on the cross section **a** the main powerhouse **b** the main transformer room
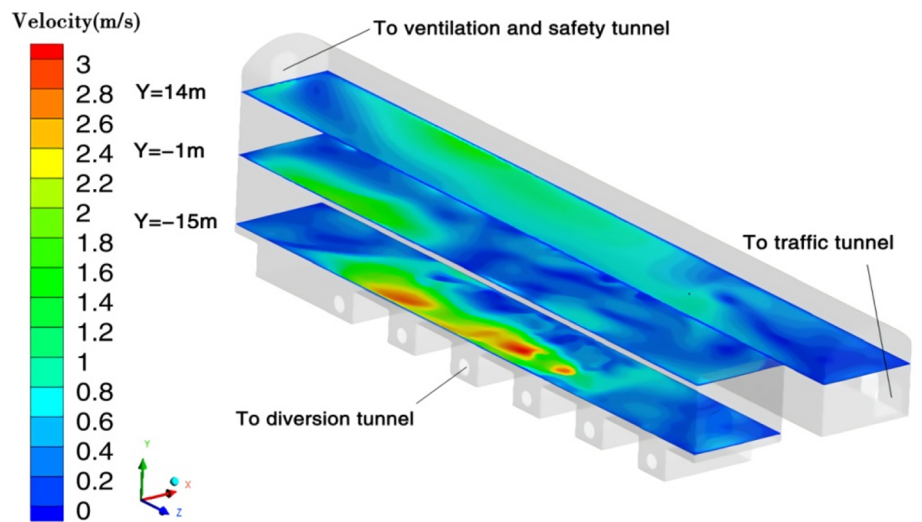
(a) the main powerhouse
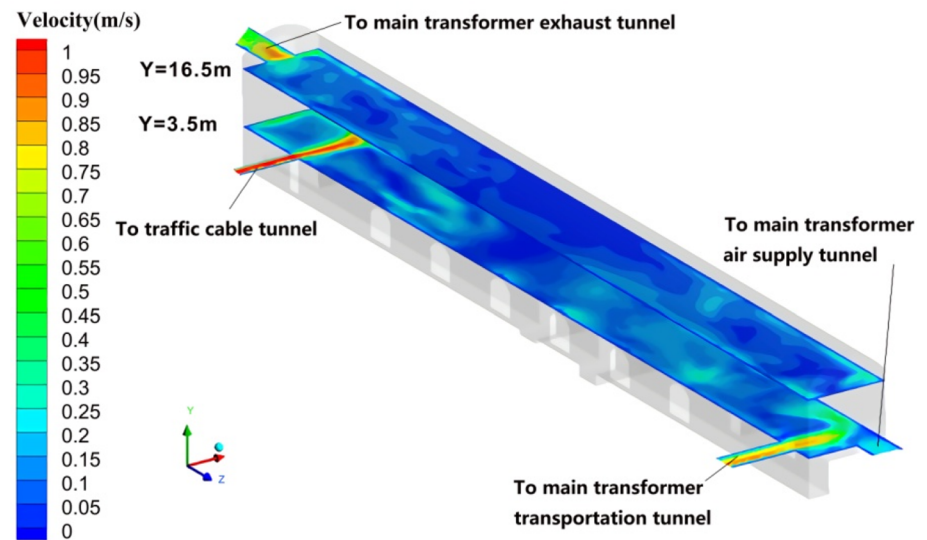
(b) the main transformer room

model established in this paper. The average relative errors of feature points 1–8 are all less than 10%, and the simulation results of feature points 9 and 10 have large errors. However, the average relative errors of the two measurement points are also less than 15%, which is within the allowable error range. From the velocity vector distribution in Fig. 12, the simulation errors of the feature point 9 and 10 are large mainly because there are two opposite directions of airflow near the feature points, then converge and flow into the ventilation shaft, disturbing each other and making the airflow unevenly distributed. Moreover, it is directly affected by natural airflow from the entrance of the ventilation and

safety cavern, and the velocity fluctuates slightly, leading to a certain difference between the simulated value and the measured value.

6 Conclusion

The paper applies CFD analysis method to establish a numerical model for the underground cavern group of a pumped storage power station and studies the influence characteristics of the ventilation shaft diameter and inclination
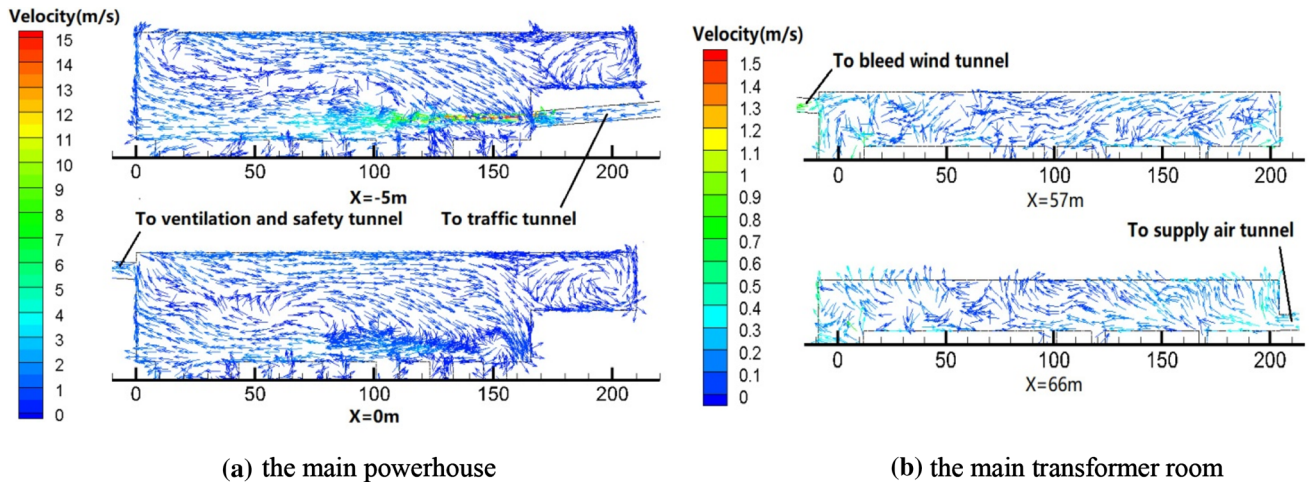
(a) the main powerhouse

(b) the main transformer room

Fig. 9 Velocity vector on the cross section **a** the main powerhouse **b** the main transformer room

(a) The main powerhouse

(b) The main transformer room
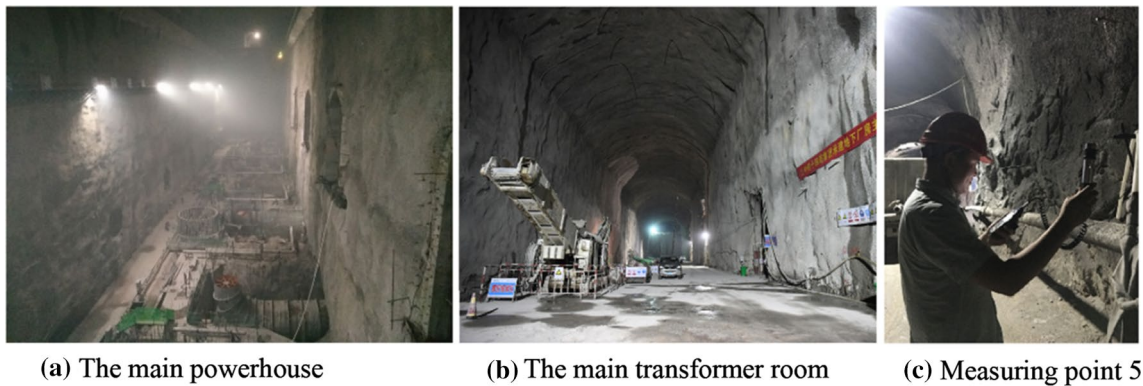
(c) Measuring point 5

Fig. 10 Construction and test site **a** The main powerhouse **b** The main transformer room **c** Measuring point 5
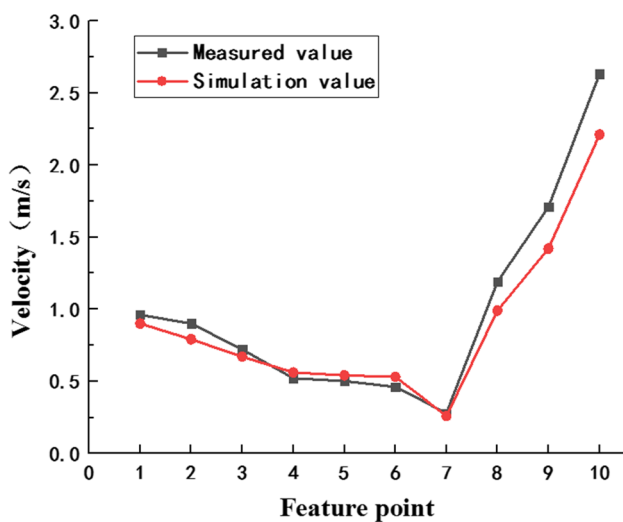

Fig. 11 Comparison of airflow velocity between field data and simulated result

on the ventilation flow field. Combined with the field test data, the following main conclusions are obtained:

(1) The influence of the airflow in the main caverns and the distribution of air velocity under different ventilation shaft diameters is studied. Compared with the main powerhouse, the change of the ventilation shaft diameter has a limited impact on the ventilation in the main transformer tunnel. When the diameter of the ventilation shaft is 8 m, the average air speed near the ground of the main powerhouse can be increased to 1.09 m/s, and the speed unevenness coefficient is 0.64. The air field distribution is relatively uniform, and the ventilation effect is the most ideal.

(2) When the inclination angle of the ventilation shaft is 80°, the jet flow of the inlet fan in the main building can reach the farthest diffusion distance, and the wind speed dissipation loss is the smallest, which is beneficial
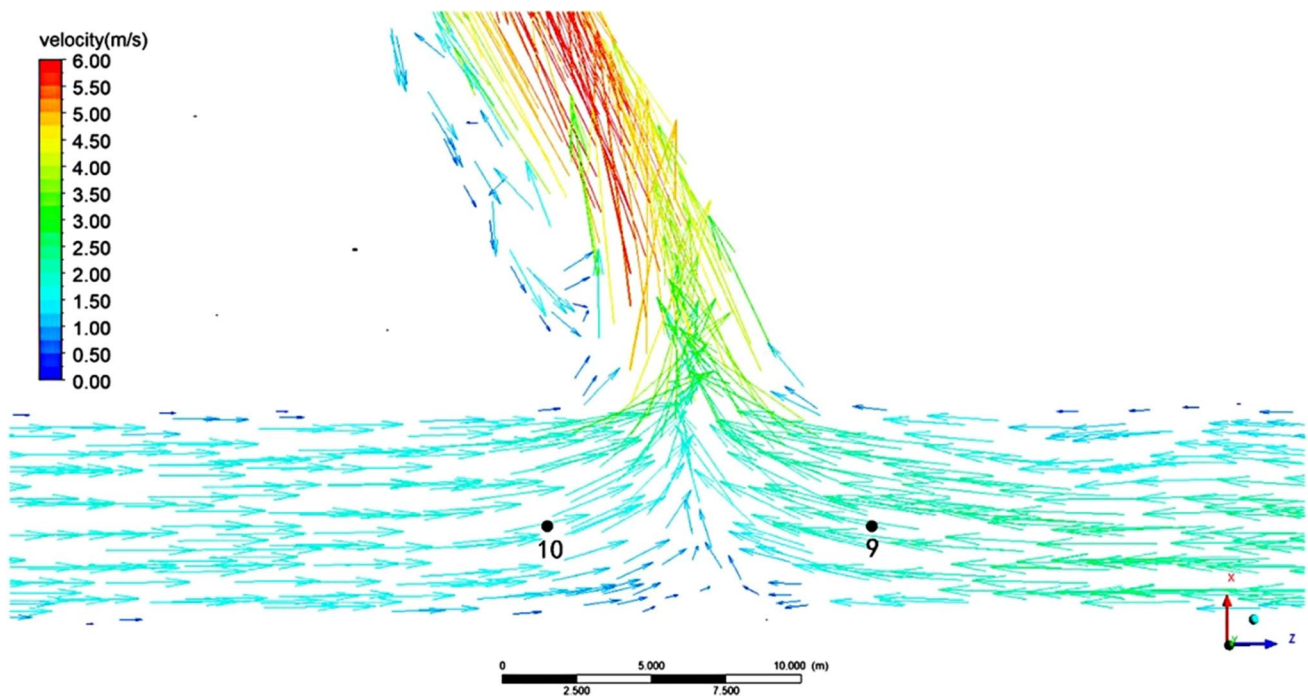
Fig. 12 Velocity distribution at measuring points 9 and 10

to increase the wind speed in the tunnel and speed up the air replacement. At the same time, the speed unevenness coefficients in the main powerhouse and the main transformer tunnel are also low, respectively 0.65 and 0.72. The uniformity of the velocity field distribution is better, and the ventilation effect in the underground cavern group is better than other working conditions.

(3) Combined with the above numerical analysis results, the ventilation effect under the shaft diameter of 8 m and the inclination angle of 80° is studied. The simulation results show that the airflow in the underground cavern group under this scheme is orderly, the main powerhouse and the main transformer tunnel can form a "bottom in and top out" replacement flow, and the air speed generally meets the requirements of the specification. Finally, this scheme is used in engineering practice, and the field measured data is compared with the simulation value. The experimental value is very consistent with the CFD simulation value, and the average relative error is 11.32%. Therefore, it shows that the used CFD method can be applied to the performance prediction and evaluation of the complex underground cavern group ventilation system.

References

1. Li, Y.L.; Yin, Q.; Mo, Z.Y.; Tang, C.Z.; Chen, X.; Yang, X.G.: Optimization of construction ventilation scheme for large-scale underground cavern group of Xiangjiaba hydropower station based on numerical simulation. J. Sichuan Univ. (Eng. Sci. Edition). **42**(04), 1–6 (2010)
2. Li, M.; Aminossadati, S.M.; Wu, C.: Numerical simulation of air ventilation in super-large underground developments. Tunn. Undergr. Space Technol. **52**, 38–43 (2016)
3. Tong, Y.; Shi, M.H.; Gong, Y.F.; He, J.P.: Full-scale experimental study on smoke flow in natural ventilation road tunnel fires with shafts. Tunn. Undergr. Space Technol. **24**(6), 627–633 (2009)
4. Zhong, M.; Shi, C.; He, L.; Shi, J.; Fu, T.: Full-scale experimental research on fire fume refluence of sloped long and large curved tunnel. SCIENCE CHINA Technol. Sci. **54**(S1), 89–94 (2011)
5. Zhong, M.; Shi, C.; He, L.; Shi, J.; Liu, C.; Tian, X.: Smoke development in full-scale sloped long and large curved tunnel fires under natural ventilation. Appl. Therm. Eng. **108**, 857–865 (2016)
6. Sun, J.; Fang, Z.; Chen, J.: Full-scale experiment of longitudinal ventilation smoke control system and central smoke exhaust

system in city underwater tunnel. Procedia Engineering. **52**, 330–335 (2013)

7. Pflitsch, A.; Bruene, M.; Steiling, B.; Killing-Heinze, M.; Agnew, B.; Irving, M.; Lockhart, J.: Air flow measurements in the underground section of a UK light rail system. Appl. Therm. Eng. **32**, 22–30 (2012)

8. Musto, M.; Rotondo, G.: Numerical comparison of performance between traditional and alternative jet fans in tiled tunnel in emergency ventilation. Tunn. Undergr. Space Technol. **42**, 52–58 (2014)

9. Nan, C.; Ma, J.; Luo, Z.; Zheng, S.; Wang, Z.: Numerical study on the mean velocity distribution law of air backflow and the effective interaction length of airflow in forced ventilated tunnels. Tunn. Undergr. Space Technol. **46**, 104–110 (2015)

10. Lee, S.C.; Lee, S.; Lee, J.: CFD analysis on ventilation characteristics of jet fan with different pitch angle. KSCE J. Civ. Eng. **18**(3), 812–818 (2014)

11. Diego, I.; Torno, S.; Toraño, J.; Menéndez, M.; Gent, M.: A practical use of CFD for ventilation of underground works. Tunn. Undergr. Space Technol. **26**(1), 189–200 (2011)

12. Wang, X.; Zhang, Z.; Zhou, Z.; Chen, H.: Numerical simulation of TBM construction ventilation in a long diversion tunnel. Tunn. Undergr. Space Technol. **26**(4), 560–572 (2011)

13. Sa, Z.; Li, F.; Qin, B.; Pan, X.: Numerical simulation study of dust concentration distribution regularity in cavern stope. Saf. Sci. **50**(4), 857–860 (2012)

14. Zhang, H.; Sun, J.; Lin, F.; Chen, S.; Yang, J.: Optimization scheme for construction ventilation in large-scale underground oil storage caverns. Appl. Sci. **8**(10), 1652 (2018)

15. Lin, F.: Construction network ventilation system for underground lpg storage cavern. Civil Eng. J. **4**(7), 1521–1541 (2018)

16. Hua, T.B.; Wang, Y.S.; Yao, Q.; Yang, X.G.; Li, H.T.: Numerical simulation and detection feedback of ventilation in the surge-chamber of a hydropower station. Adv. Eng. Sci. **49**(03), 29–36 (2017)

17. Zhang, H.; Lin, F.; Zhang, K.; Yang, J.S.; Chen, S.G.: Establishment of a ventilation network and the shaft ventilation effect in a large underground cavern group. Modern Tunn. Technol. **55**(01), 203–209 (2018)

18. Liu, Y.; Wang, S.; Deng, Y.; Ma, W.; Ma, Y.: Numerical simulation and experimental study on ventilation system for power-houses of deep underground hydropower stations. Appl. Therm. Eng. **105**, 151–158 (2016)

19. Liu, Z.; Wang, X.L.; Zhang, A.L.: Construction ventilation scheme optimization of underground main powerhouse based on CFD. Appl. Mech. Mater. **368–370**, 619–623 (2013)

20. Lateb, M.; Masson, C.; Stathopoulos, T.; Bédard, C.: Comparison of various types of k–ε models for pollutant emissions around a two-building configuration. J. Wind Eng. Ind. Aerodyn. **115**, 9–21 (2013)

21. Nan, C.Z.; Zhang, W.H.; Zhao, X.; Zhou, Y.L.; Ma, J.M.: Numerical simulations of ventilation to remove noxious gases during excavation of complicated tunnels. J. Tsinghua Univ. (Sci. Technol.). **54**(08), 993–998 (2014)

22. Qiao, L.: Optimization of structural setting based on forced ventilation method in tunnel under construction. J. Southwest Jiaotong Univ. **53**(06), 1245–1252 (2018)

23. Zhang, H.; Lin, F.; Sun, J.C.; Zhou, Z.L.; Zhang, H.; Lin, F.: CFD analysis of ventilation effect of tunnel construction based on typical wall rough model. China Railway Sci. **37**(5), 58–65 (2016)

24. Shao, S.; Yang, X.G.; Zhou, J.W.: Numerical analysis of different ventilation schemes during the construction process of inclined tunnel groups at the Changheba Hydropower Station, China. Tunn. Underground Space Technol. incorporating Trenc. Technol. Res. **59**, 157–169 (2016)

25. Li, A.; Ren, T.; Yang, C.; Xiong, J.; Tao, P.: Numerical simulation, PIV measurements and analysis of air movement influenced by nozzle jets and heat sources in underground generator hall. Build. Environ. **131**, 16–31 (2017)

26. Tao, P.; Li, A.; Zhang, J.; Wang, J.: Scaling model study of the air distribution in a powerhouse under different ventilation conditions. Build. Simul. **7**(4), 389–400 (2014)

27. Li, A.; Tao, P.; Bao, X.; Zhao, Y.: PIV measurements of air distribution in a reduced-scale model - ventilation of a busbar corridor in a hydropower station. Int. J. Vent. **12**(1), 81–98 (2013)

28. Shao, S.; Yang, X.; Zhou, J.: Numerical analysis of different ventilation schemes during the construction process of inclined tunnel groups at the Changheba Hydropower Station. China. Tunnelling and Underground Space Technology. **59**, 157–169 (2016)

29. Wu, Y.; Shi, X.C.; Han, H.; Gao, X.Q.: Numerical simulation for contaminant dispersion induced by human-walking at the gateway of civil protection engineering. J. Saf. Environ. **14**(02), 208–213 (2014)